Ground motion prediction maps including site effects for Near-Real-Time Assessment of Seismically Induced Landslide.

Acunzo G., **Falcone G.**, Mendicelli A., Mori F., Moscatelli M., Naso G.

05 November 2021

Summary

- Introduction: ground shaking, from source to local site effects
- Key dynamic properties and seismic effects national maps: V_{S30}, Amplification Factors
- Ground motion prediction maps
- Conclusions
- What's next?

Summary

- **Introduction: ground shaking, from source to local site effects**
- Key dynamic properties and seismic effects national maps: V_{S30}, Amplification Factors
- Ground motion prediction maps
- Conclusions
- What's next?

Introduction:
ground shaking, from source to local site effects

Ground motion: ground motion recorded at a reference site (outcropping stiff rock characterised by a flat ground surface), in general, differs from the ground motion recorded at a site of interest due to local stratigraphic condition, buried morphology, and topography.

Seismic induced phenomena: ground motion variation over small areas, subsidence, liquefaction, and landslides.

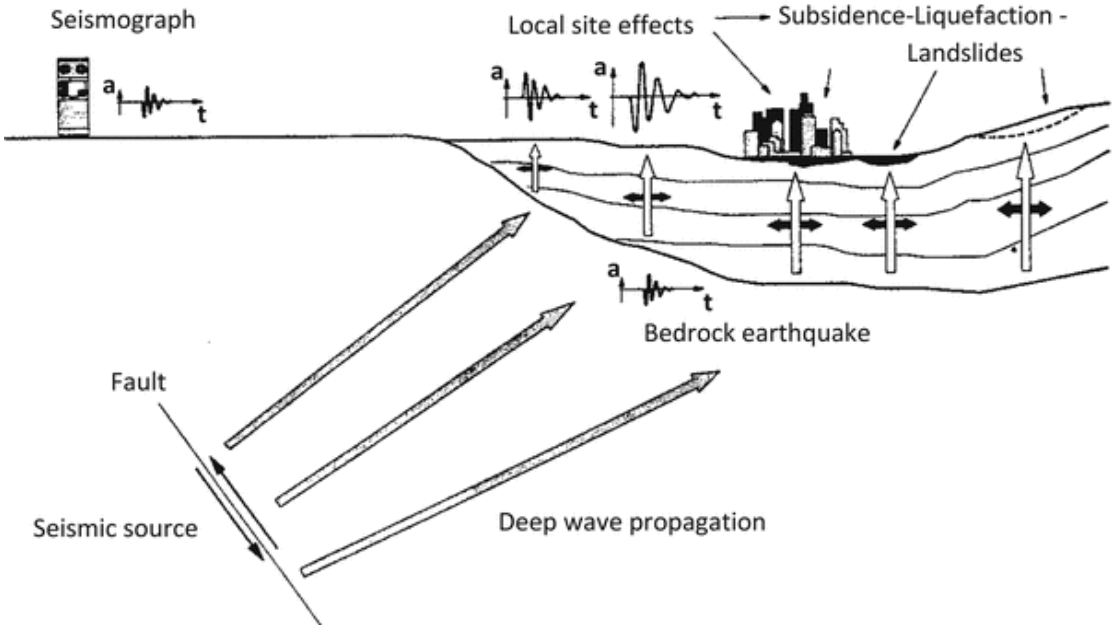

(from Kramer S.L., 1996)

Ground motion prediction over small areas is based on a detailed subsoil model and a proper characterization of mechanical soil response. In addition, the topography should be considered in the model. Moreover, an input motion should be retrieved from a proper hazard analysis considering the seismic source of interest (*Kramer, 1996*). Hence, numerical simulation of seismic site response is performed providing detailed output (e.g., acceleration time history, pseudo-acceleration response spectra, and so on).

On the other hand, **Ground motion prediction over large areas**, is based on key parameters which provide the mechanical response of soil, the subsoil setting, and the topography of the area of interest in a synthetic way. A reliable list of synthetic parameters is (*Zhou et al., 2020; Mori et al., 2021*):

- mean shear wave velocity in the upper 30 m of the soil deposit (V_{S30});
- fundamental frequency (f_0) and thickness (H_{cover}) of the cover deposit;
- elevation (H);
- slope (s);
- topographic gradients (h_x and h_y, where x and y are two orthogonal directions);
- second-order topographic gradients (h_{xx} and h_{yy}).

Finally, the seismic source condition can be considered in terms of magnitude (M) and epicentral distance (R).

Introduction: ground motion prediction, key parameters

Ground motion prediction over small areas is based on a detailed subsoil model and a proper characterization of mechanical soil response. In addition, the topography should be considered in the model. Moreover, an input motion should be retrieved from a proper hazard analysis considering the seismic source of interest (*Kramer, 1996*). Hence, numerical simulation of seismic site response is performed providing detailed output (e.g., acceleration time history, pseudo-acceleration response spectra, and so on).

On the other hand, **Ground motion prediction over large areas**, is based on key parameters which provide the mechanical response of soil, the subsoil setting, and the topography of the area of interest in a synthetic way. A reliable list of synthetic parameters is (*Zhou et al., 2020; Mori et al., 2021*):

- mean shear wave velocity in the upper 30 m of the soil deposit (V_{S30});
- fundamental frequency (f_0) and thickness (H_{cover}) of the cover deposit;
- elevation (H);
- slope (s);
- topographic gradients (h_x and h_y, where x and y are two orthogonal directions);
- second-order topographic gradients (h_{xx} and h_{yy}).

Finally, the seismic source condition can be considered in terms of magnitude (M) and epicentral distance (R).

Maps of synthetic parameters are required to predict ground motion over large areas

Summary

- Introduction: ground shaking, from source to local site effects
- **Key dynamic properties and seismic effects national maps: V_{S30}, Amplification Factors**
- Ground motion prediction maps
- Conclusions
- What's next?

V_{S30} map of Italy

1) V_S and lithological data were retrieved from about 11'000 *in situ* investigations (DH, MASW, and continuous boreholes from Italian Seismic Microzonation Studies available at *https://www.webms.it/*);
2) V_S and lithological data were grouped according to 40 morpho-geological (*Iwahashi et al., 2018*) and 2 lithological clusters;
3) A multilinear regression model was performed for each cluster:

$$\ln(V_{S30}) = c_0 + c_1 \cdot \ln(s) + c_2 \cdot \ln(H)$$

where s and H are slope and elevation, respectively.

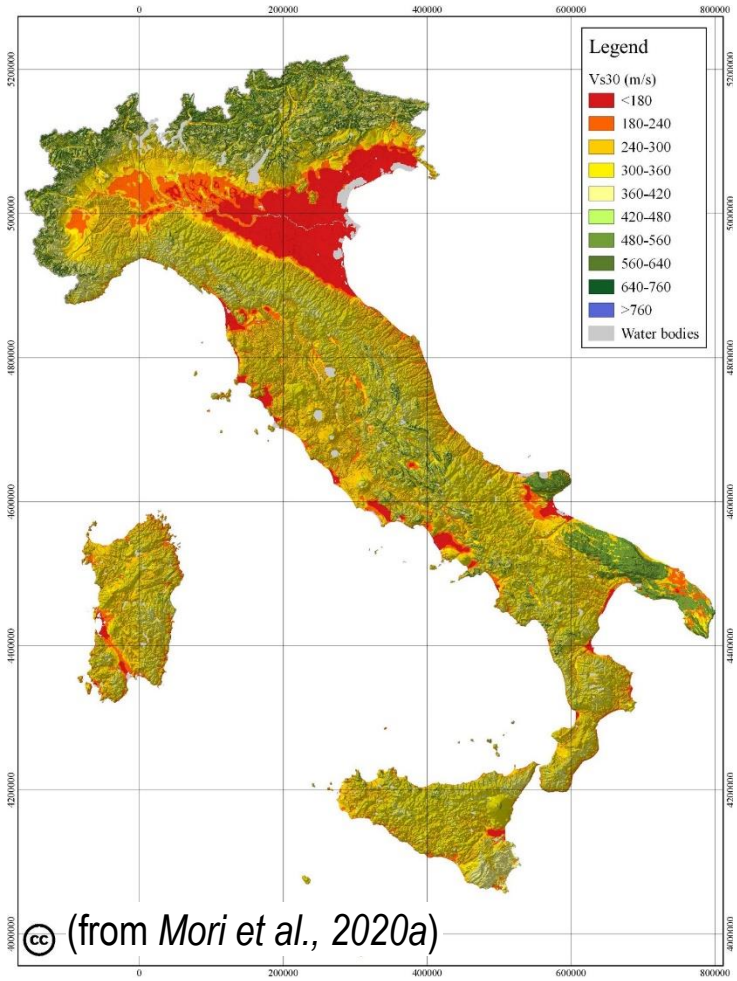

(from *Mori et al., 2020a*)

Amplification Factor map of Italy

1) V_S and lithological data were retrieved from about 16'000 and 44'000, respectively, *in situ* investigations (DH, MASW, and continuous boreholes from Italian Seismic Microzonation Studies available at *https://www.webms.it/*);

2) About 2 millions of V_S profiles were provided basing on a stochastic procedure and grouped according to 40 morpho-geological (*Iwahashi et al., 2018*) and 2 lithological clusters;

3) Reference motions were selected according with the Italian Seismic Hazard (*http://esse1.mi.ingv.it/d2.html*) with reference to 475 years as return period;

4) About 30 million of numerical simulations of seismic site response were performed;

5) A regression model was suggested for each cluster depending on the intensity of the reference motion:

$$\ln(AF) = c_0 + c_1 \cdot \ln^2(V_{S30}) + c_2 \cdot \ln(V_{S30})$$

where AF is the amplification factor.

$$AF_{T_1\text{-}T_2} = \frac{\int_{T_1}^{T_2} Sa_o dT}{\int_{T_1}^{T_2} Sa_i dT}$$

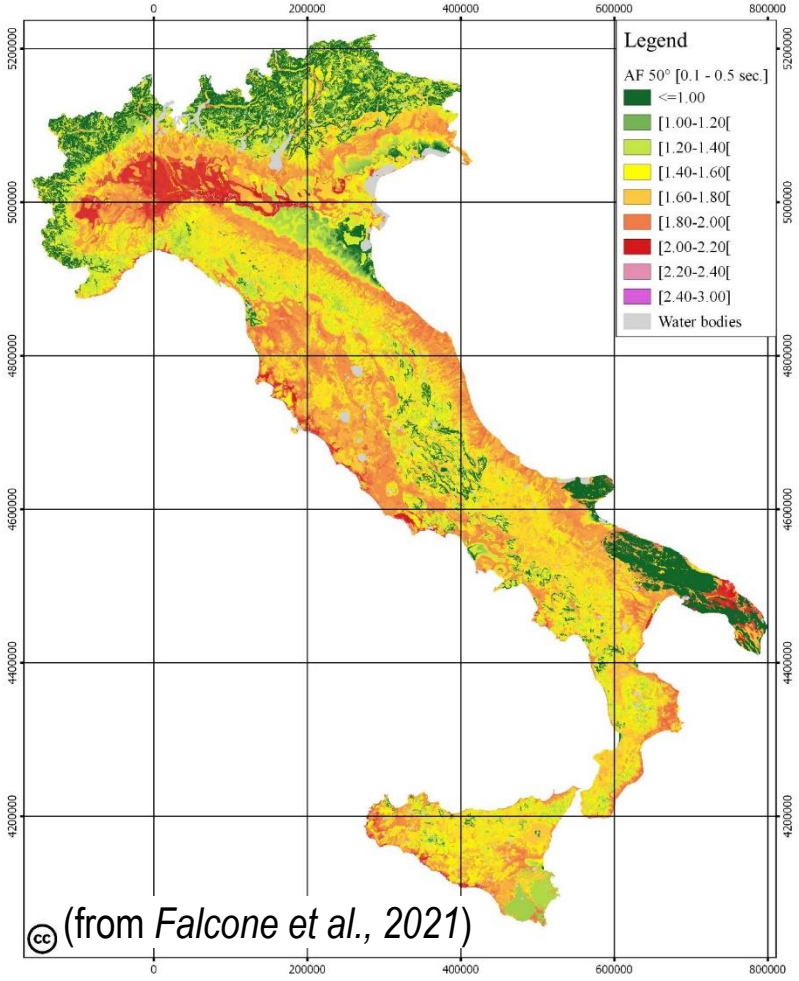

(from *Falcone et al., 2021*)

AF and V_{S30} maps as input layer for seismic induced phenomena

Maps of key parameters (e.g., V_{S30}) and amplification factors can be considered to outweigh permanent ground deformation phenomena (e.g., liquefaction and slope movements). For instance, logistic regression models were considered. Machine learning procedure will be provided in the future.

The probability of landslide occurrence is given by:

$$P(X) = 1/(1 + e^{-t})$$

$$t = k_0 + k_1 \cdot ln(PGV) + k_2 \cdot slope + k_3 \cdot lithology + k_4 \cdot landcover + k_5 \cdot CTI + k_6 \cdot ln(PGV) \cdot slope$$

(*Nowicki et al., 2018*)

The probability of liquefaction occurrence is given by:

$$P(X) = 1/(1 + e^{-t}) = k_0 + k_1 \cdot ln(PGV) + k_2 \cdot \ln(V_{s,30}) + k_3 \cdot precip + k_4 \cdot dw + k_5 \cdot wtd$$

(*Zhu et al., 2017*)

where PGV was determined considering the local site effects (i.e., reference motion modified by the amplification factors).

Probability of landslide triggered by earthquake

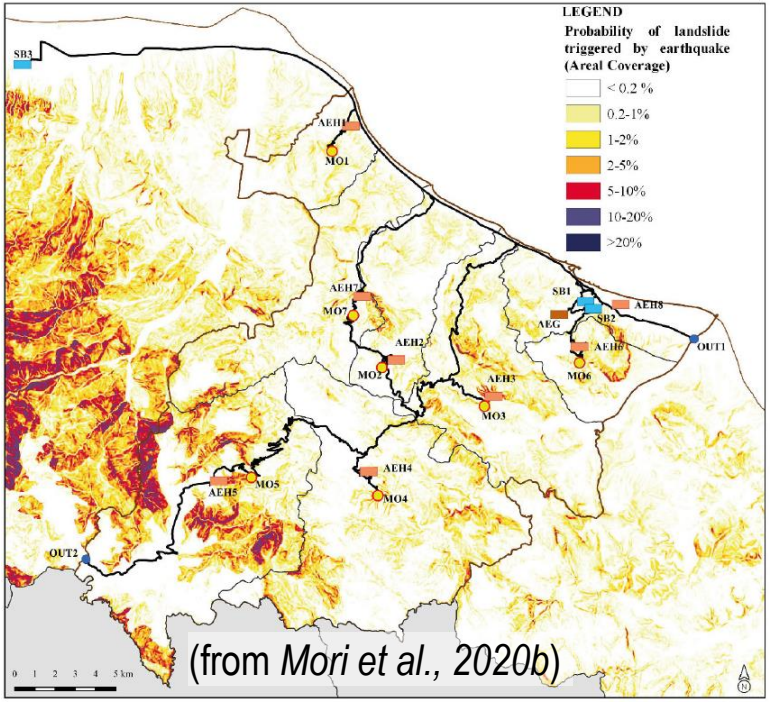

(from *Mori et al., 2020b*)

Summary

- Introduction: ground shaking, from source to local site effects
- Key dynamic properties and seismic effects national maps: V_{S30}, Amplification Factors
- **Ground motion prediction maps**
- Conclusions
- What's next?

Ground motion prediction maps aims

A ML procedure was selected to provide near-real-time ground motion prediction maps to support emergency management system. The paradigm was shifted from the evaluation of amplification factors to the evaluation of the ground motion variation over large areas directly including local site effects.

In detail, ML approach was adopted to:

i) implement source parameters (H, R, and M) available few minutes after a seismic event;

ii) include both lithostratigraphic (V_{S30}) and morphological (h, h_x, h_y, h_{xx}, h_{yy}) key parameters;

iii) provide maps of intensity measure (peak ground velocity, peak ground acceleration, and spectral acceleration at 0.3 s, 1.0 s and 3.0 s) over large areas few minute after an earthquake;

iv) capture the spatial variation at short distances (hundreds of meters) due to local site effects, which is essential for reliable hazard assessments.

Input and output data of the ML procedure

Type of data	Category		Control Factors	Database	Ref.
INPUT	Seismological	H	hypocentral depth	Seismological DB	Luzi et al., 2016 and 2020
		M	moment magnitude		
		R	epicentral distance		
	Geophysical	V_{S30}	the time-averaged shear-wave velocity to 30 m depth	Seismological DB or V_{S30} map	Luzi et al., 2016 and 2020 DPC, 2018 Mori et al., 2020b
	Morphological	h	elevation	ALOS World 3D-30m DEM	http://www.eorc.jaxa.jp/ALOS/en/aw3d30/
		h_x	first order partial derivative dx (E-W slope)		
		h_y	first order partial derivative dy (N-S slope)		
		h_{xx}	second order partial derivative dyy		
		h_{yy}	second order partial derivative dxx		
OUTPUT	Seismological	PGA	Peak Ground Acceleration	Seismological DB	Luzi et al., 2016 and 2020
		PGV	Peak Ground Velocity		
		$Sa_{0.3}$	Spectral acceleration at 0.3 s		
		$Sa_{1.0}$	Spectral acceleration at 1 s		
		$Sa_{3.0}$	Spectral acceleration at 3 s		

Selection of the ML procedure

The "Matlab Regression Learner App" tool (*https://it.mathworks.com/help/stats/regression-learner-app.html*) was employed to produce ground motion prediction maps using a supervised ML approach. The desired model among many different methods was chosen as characterized by the best performance in terms of RMSE.

	Performance in term of RMSE				
ML Prediction Model	**PGA**	**PGV**	**Sa(0.3s)**	**Sa(1.0s)**	**Sa(3.0s)**
Linear Regression (Linear)	0.53	0.47	0.50	0.44	0.43
Linear Regression (Interactions Linear)	0.48	0.43	0.47	0.42	0.40
Linear Regression (Robust Linear)	0.53	0.47	0.50	0.44	0.43
Stepwise Linear Regression (Stepwise Linear)	0.48	0.43	0.47	0.42	0.40
Tree (Fine Tree)	0.42	0.38	0.42	0.39	0.38
Tree (Medium Tree)	0.40	0.36	0.40	0.38	0.36
Tree (Coarse Tree)	0.40	0.36	0.40	0.37	0.36
Support Vector Machine (Linear)	0.53	0.48	0.49	0.44	0.43
Support Vector Machine (Quadratic)	0.43	0.39	0.42	0.39	0.39
Support Vector Machine (Cubic)	0.40	0.36	0.40	0.37	0.36
Support Vector Machine (Fine Gaussian)	0.48	0.46	0.48	0.45	0.46
Support Vector Machine (Medium Gaussian)	0.37	0.34	0.38	0.35	0.34
Support Vector Machine (Coarse Gaussian)	0.43	0.39	0.42	0.39	0.38
Ensemble (Boosted Trees)	0.40	0.36	0.40	0.37	0.36
Ensemble (Bagged Trees)	0.33	0.31	0.33	0.31	0.31
Gaussian Process Regression (Squared Exponential)	0.38	0.35	0.39	0.36	0.35
Gaussian Process Regression (Matern 5/2)	0.37	0.34	0.38	0.34	0.34
Gaussian Process Regression (Exponential)	**0.31**	**0.30**	**0.33**	**0.30**	**0.29**

The Gaussian Process Regression (GPR) was selected to produce ground motion prediction maps.

The mean and standard deviation (std) values of the residuals' distribution was quantified and compared with available literature data.

It is worth noting that the suggested ML approach provides the best performance with respect to the approaches proposed by the other studies in terms of both accuracy (mean value) and precision (standard deviation). In detail, the standard deviation values are reduced by the 45-60%.

$$\text{residual} = \log_{10}\left(\frac{\text{IM}_{\text{observed}}}{\text{IM}_{\text{predicted}}}\right)$$

IM (geoH)	This study (ML)		ShakeMap *		GMPE *	
	mean	std	mean	std	mean	std
PGA	-0.000033	0.161	0.038	0.372	0.017	0.352
PGV	-0.000015	0.156	0.041	0.380	-0.151	0.330
$Sa_{0.3}$	0.000024	0.192	0.046	0.370	-0.252	0.359
$Sa_{1.0}$	0.000028	0.160	0.017	0.374	-0.198	0.303
$Sa_{3.0}$	-0.000072	0.159	-0.012	0.404	0.083	0.368

* Mean and standard deviation of the residuals' distributions referred to ShakeMap and GMPE were retrieved from the work of *Jozinović et al. (2021)*.

Ground motion prediction maps

The adopted GPR model was used to produce ground motion prediction maps referring to the Central Italy earthquake occurred on August 24, 2016.

The maps show an output that is in good agreement with the geological and geomorphological characteristics of the territory and, therefore, highlights local site effects. In fact, it can be noted that the highest $Sa_{0.3}$ values well describe the valleys' trend (i.e., the largest and continuous Tronto River valley) and the two extended areas in the southern part of the map (i.e., near Petrana and Torrita villages), which are characterized by lowest values of V_{S30} (*Mori et al., 2020a*).

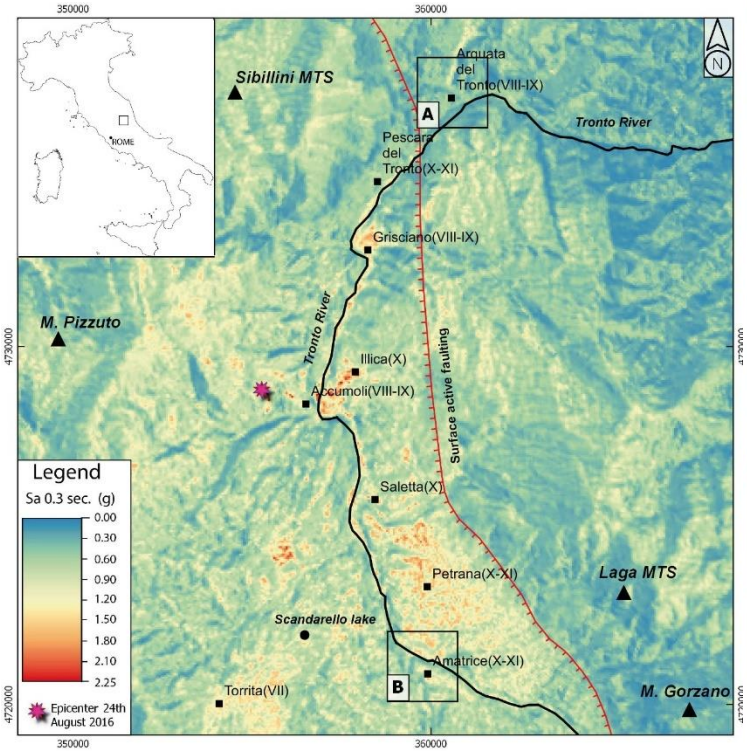

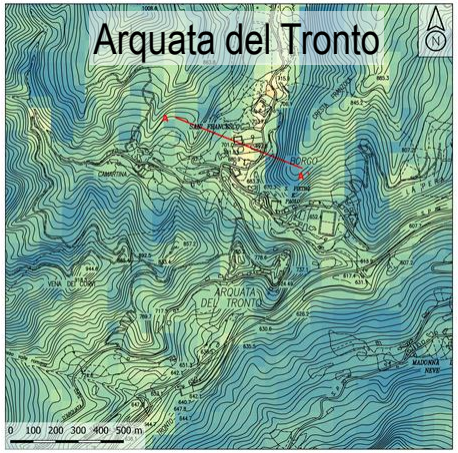

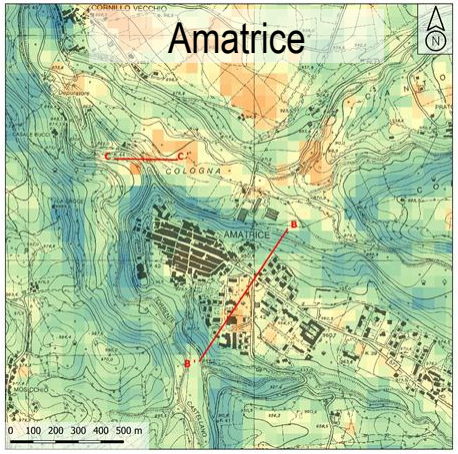

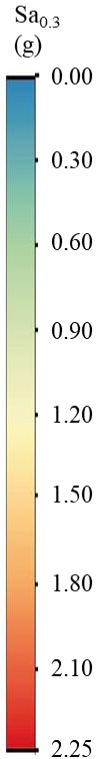

Ground motion prediction maps vs numerical simulation

With reference to AA', BB', and CC' tracks, the $Sa_{0.3}$ values from ML procedure were compared to results from site-specific numerical simulations (*Gaudiosi et al., 2021; Giallini et al., 2020; Grelle et al., 2020*) and the constant value from ShakeMap (http://shakemap.rm.ingv.it/shake4/), which fails to grasp the local site effects at this scale.

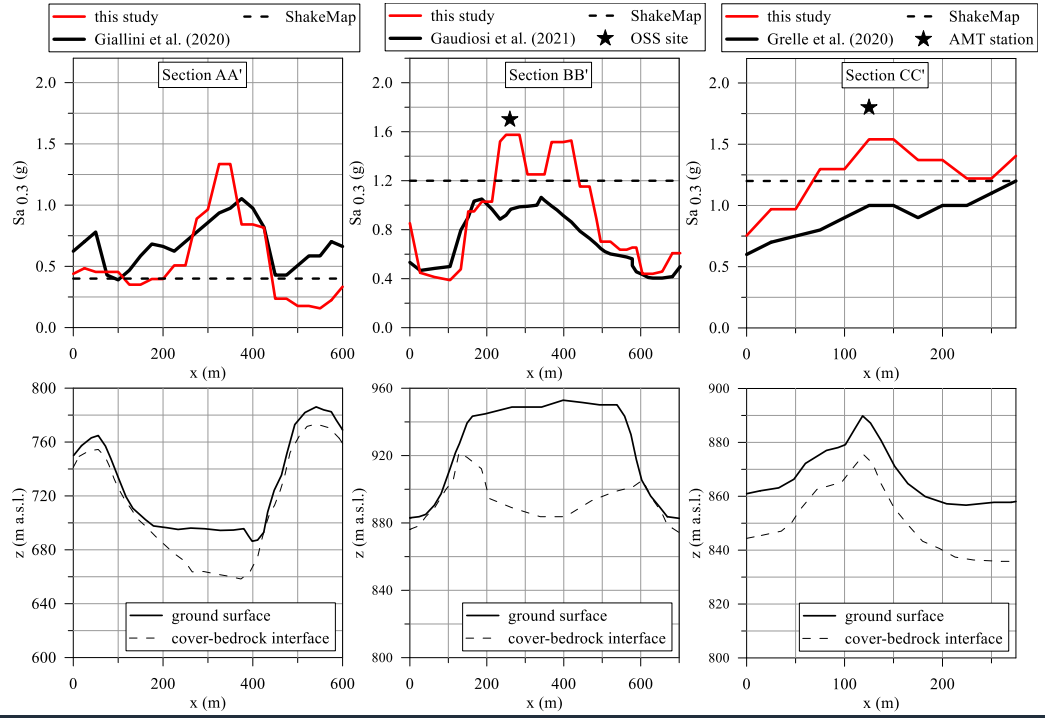

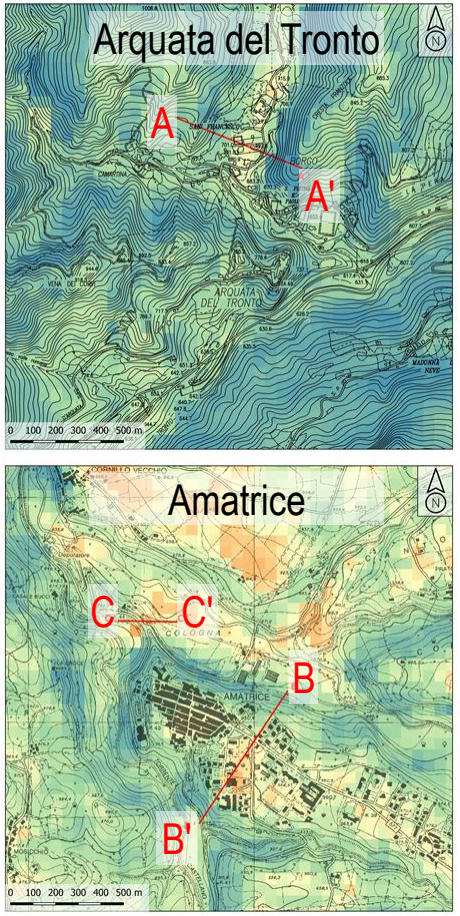

Summary

- Introduction: ground shaking, from source to local site effects
- Key dynamic properties and seismic effects national maps: V_{S30}, Amplification Factors
- Ground motion prediction maps
- **Conclusions**
- **What's next?**

Conclusions

- Italian maps of mean shear wave velocity in the upper 30 m of the deposit (V_{S30}) and of amplification factors (AF) were produced considering morpho-geological clustering and site data (about 11'000 geophysical surveys and 44'000 continuous boreholes) from the Italian database of seismic microzonation studies.
- V_{S30} and AF maps were considered to provide probability of landslide triggered by earthquake and of liquefaction based on regression logistic models over large areas.
- Ground motion prediction maps (peak ground acceleration, peak ground velocity, and spectral acceleration at 0.3 s, 1.0 s, and 3.0 s) were provided using a supervised Machine Learning approach (Gaussian Process Regression).

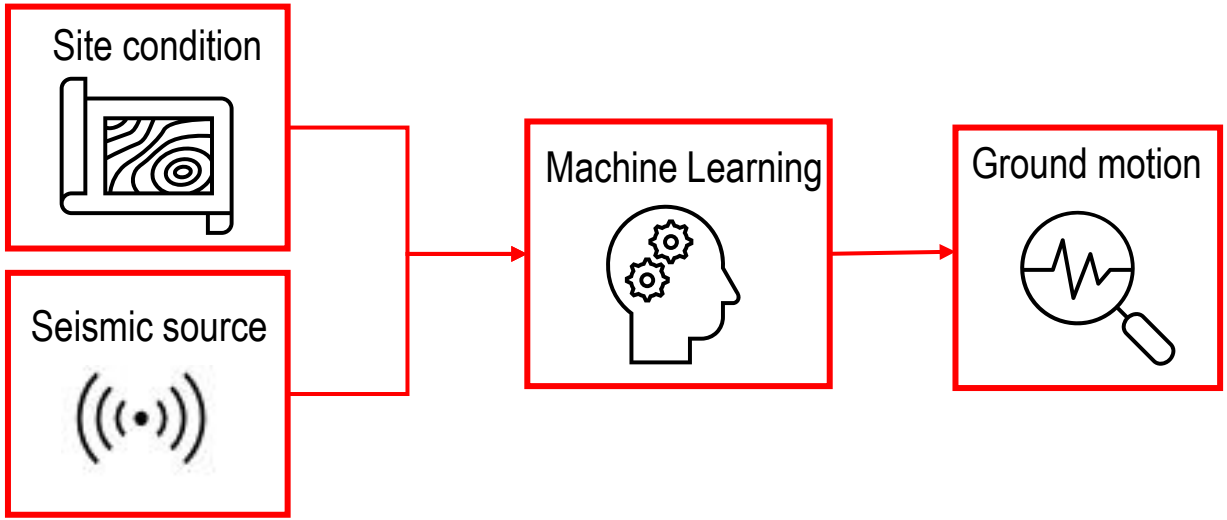

What's next?

- Produce maps of other key soil parameters (fundamental frequency and thickness of the cover deposit).
- Improve ground motion prediction maps including new key soil parameters to describe site conditions.
- Provide a Machine Learning procedure to predict earthquake triggered phenomena (e.g., co-seismic slope failure) including site conditions and ground motion retrieved from previous maps.

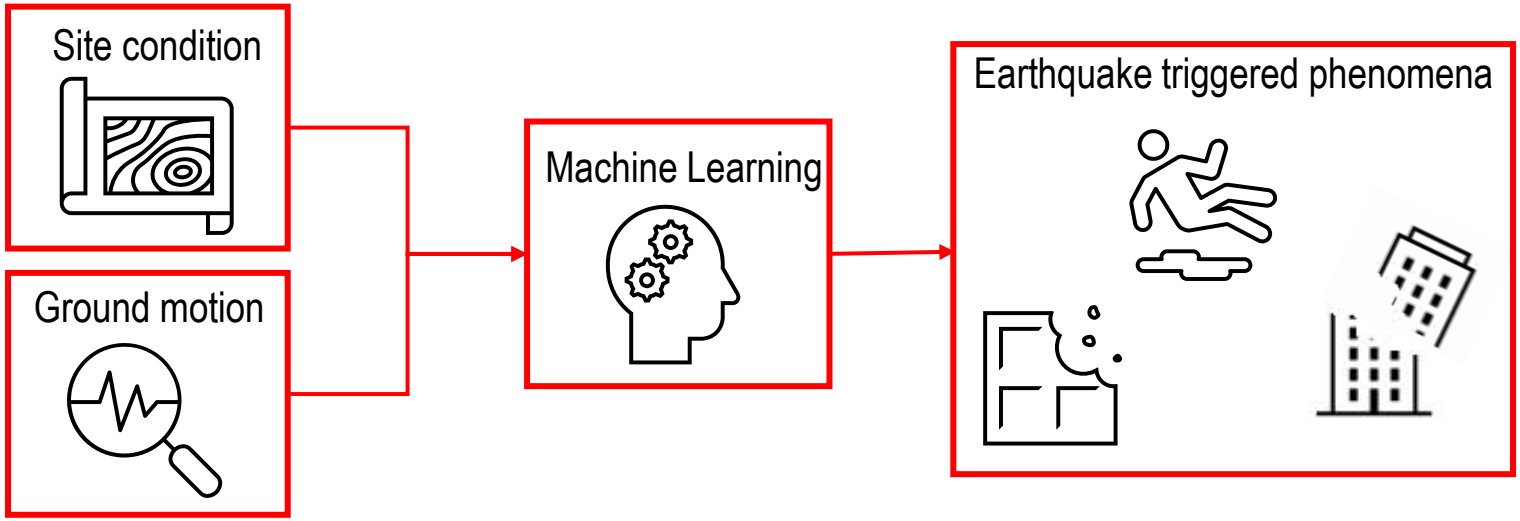

The Working Group

References

DPC, Dipartimento della Protezione Civile: Commissione tecnica per il supporto e monitoraggio degli studi di Microzonazione Sismica (ex art.5, OPCM3907/10), (2018) – WebMs; WebCLE. A cura di: M. S. Benigni, F. Bramerini, G. Carbone, S. Castenetto, G. P. Cavinato, M. Coltella, M. Giuffrè, M. Moscatelli, G. Naso, A. Pietrosante, F. Stigliano. www.webms.it.

Falcone G., Acunzo G., Mendicelli A., Mori F., Naso G., Peronace E., Porchia A., Romagnoli G., Tarquini E., Moscatelli M. (2021). Seismic amplification maps of Italy based on site-specific microzonation dataset and one-dimensional numerical approach. Eng. Geol. 289, 106170. https://doi.org/10.1016/j.enggeo.2021.106170.

Gaudiosi I., Simionato M., Mancini M., Cavinato G. P., Coltella M., Razzano R., Sirianni P., Vignaroli G. and Moscatelli M. (2021). Evaluation of site effects at Amatrice (central Italy) after the August 24th, 2016, Mw 6.0 earthquake, Soil Dyn. Earthq. Eng., 144, 106699, doi:10.1016/j.soildyn.2021.106699.

Giallini S., Pizzi A., Pagliaroli A., Moscatelli M., Vignaroli G., Sirianni P., Mancini M. and Laurenzano G. (2020). Evaluation of complex site effects through experimental methods and numerical modelling: The case history of Arquata del Tronto, central Italy, Eng. Geol., 272, 105646, doi:10.1016/j.enggeo.2020.105646.

Grelle G., Gargini E., Facciorusso J., Maresca R. and Madiai C. (2020). Seismic site effects in the Red Zone of Amatrice hill detected via the mutual sustainment of experimental and computational approaches, Bull. Earthq. Eng., 18(5), 1955–1984, doi:10.1007/s10518-019-00777-z.

Iwahashi J., Kamiya I., Matsuoka M., Yamazaki D. (2018). Global terrain classification using 280 m DEMs: segmentation, clustering, and reclassification. Prog. Earth Planet. Sci. https://doi.org/10.1186/s40645-017-0157-2.

Jozinović D., Lomax A., Štajduhar I. and Michelini A. (2021). Rapid prediction of earthquake ground shaking intensity using raw waveform data and a convolutional neural network, Geophys. J. Int., 222(2), 1379–1389, doi:10.1093/GJI/GGAA233.

Kramer S.L. (1996). Geotechnical earthquake engineering. Prentice Hall, Upper Saddle River, New Jersey.

Luzi L., Puglia R., Russo E. & ORFEUS WG5 (2016). Engineering Strong Motion Database, version 1.0. Istituto Nazionale di Geofisica e Vulcanologia, Observatories & Research Facilities for European Seismology. doi: 10.13127/ESM.

References

Luzi L., Pacor F., Puglia R. (2019). Italian Accelerometric Archive v3.0. Istituto Nazionale di Geofisica e Vulcanologia, Dipartimento della Protezione Civile Nazionale, doi: 10.13127/itaca.3.0.

Luzi L., Lanzano G., Felicetta C., D'Amico M. C., Russo E., Sgobba S., Pacor, F., & ORFEUS Working Group 5 (2020). Engineering Strong Motion Database (ESM) (Version 2.0). Istituto Nazionale di Geofisica e Vulcanologia (INGV). https://doi.org/10.13127/ESM.2.

Mori F., Mendicelli A., Falcone G., Acunzo G., Spacagna R. L., Naso G., and Moscatelli M. (2021) Ground motion prediction maps using seismic microzonation data and machine learning, Nat. Hazards Earth Syst. Sci. Discuss. [preprint], https://doi.org/10.5194/nhess-2021-282, in review.

Mori F., Mendicelli A., Moscatelli M., Romagnoli G., Peronace E., Naso G., (2020a). A new Vs30 map for Italy based on the seismic microzonation dataset. Eng. Geol. 275, 105745. https://doi.org/10.1016/j.enggeo.2020.105745.

Mori F., Gena A., Mendicelli A., Naso G., Spina D. (2020b). Seismic emergency system evaluation: The role of seismic hazard and local effects. Engineering Geology 270, 105587. https://doi.org/10.1016/j.enggeo.2020.105587.

Nowicki J.M.A., Hamburger M.W., Allstadt K., Wald D.J., Robeson S.M., Tanyas H., Hearne M., Thompson M. (2018). A global empirical model for near-real-time assessment of seismically induced landslides. Journal of Geophysical Research Earth Surface 123, 1835–1859. https://doi.org/10.1029/2017JF004494.

Zhou H., Li J., and Chen X. (2020). Establishment of a seismic topographic effect prediction model in the Lushan Ms 7.0 earthquake area, Geophys. J. Int., 221(1), 273–288, doi:10.1093/gji/ggaa003.

Zhu J., Baise L.G., Thompson E.M. (2017). An updated geospatial liquefaction model for global application. Bull. Seismol. Soc. Am. 107, 3. https://doi.org/10.1785/0120160198.

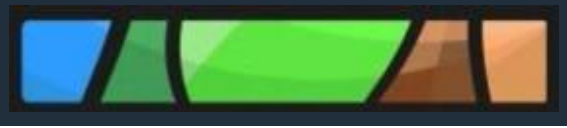

Thank you for your attention